Construction and Building Materials 174 (2018) 675–683

Contents lists available at ScienceDirect

Construction and Building Materials

journal homepage: www.elsevier.com/locate/conbuildmat

Structural behavior of corroded reinforced concrete beams under sustained loading

Weiping Zhang, Hongfei Zhang, Xianglin Gu *, Wei Liu

Key Laboratory of Performance Evolution and Control for Engineering Structures (Tongji University), Ministry of Education, Shanghai 200092, China
Department of Structural Engineering, Tongji University, Shanghai 200092, China

HIGHLIGHTS

- An experimental study on combined effects of reinforcement corrosion and sustained loads on flexural behavior of reinforced concrete beams was carried out.
- Reinforcement corrosion had a slight effect on the development of transverse crack width.
- A higher load level and a lower current density leads to more obvious deflection development of RC beams.
- The effect of reinforcement corrosion on the beam's deflection cannot be ignored.

ARTICLE INFO

Article history:
Received 14 July 2017
Received in revised form 15 April 2018
Accepted 17 April 2018

Keywords:
Corrosion
Cracking
Deflection
Reinforced concrete beam
Sustained load

ABSTRACT

This paper presents the results of an experimental study designed to investigate the combined effects of corrosion and sustained loads on the structural performance of reinforced concrete beams. A total of eight RC beams, including both uncorroded beams and corroded ones accelerated by the impressed current method, were tested. All the beams were subjected to a four-point sustained bending load which was equivalent to 17%, 33% or 50% of the designed ultimate load, respectively. Corrosion degree, crack patterns, crack width and mid-span deflection of the beams were monitored during the test. The results showed that reinforcement corrosion had no obvious effect on the transverse crack spacing and a slight effect on the development of transverse crack width for the beams under simultaneous loading and corrosion. A higher load level and a lower current density allow for more sufficient oxidation of corrosion products with a larger volume expansion rate, leading to premature initiation and rapid propagation of corrosion cracking, and more obvious deflection development of RC beams. For a beam under simultaneous loading and reinforcement corrosion, the effect of reinforcement corrosion on its deflection cannot be ignored, because it may exceed creep effect at a relatively low corrosion degree.

1. Introduction

Reinforced concrete (RC) is one of the most widely used construction materials in the world. RC structures are usually regarded as permanent structures that can be free of severe degradation problems for a long period time owing to their good service performance. Although steel bars embedded in concrete are normally protected against corrosion during the service life of a structure, the concrete cover can deteriorate under the effects of some aggressive agents, leading to corrosion of the steel bars in concrete. For RC structures, corrosion of steel bars is one of the most important factors causing durability problems [1]. On the one hand, corrosion can lead to the cross-sectional loss of steel bars and degradation of their mechanical properties thereby reducing the bearing capacity of a structural member. On the other hand, steel bars corrosion can also degrade the bonding behavior between the concrete and steel, thereby inducing stiffness reduction, which can increase the deflection during the service life.

Much research has been done on behavior of corroded RC beams. However, the most previous work has focused on the short-term behavior of corroded RC beams where the beam specimens were pre-corroded before loading to failure. Cabrera [2], Mangat et al. [3] and Torres-Acosta et al. [4] found that transverse crack width and crack spacing increased with the corrosion degree, but the quantity of cracks decreased. Actually, corrosion of steel bars normally takes place while a structure is subjected to a sustained load. The sustained load may lead to an accelerating effect

* Corresponding author.
E-mail address: gxl@tongji.edu.cn (X. Gu).

https://doi.org/10.1016/j.conbuildmat.2018.04.145
0950-0618/

List of notations

A	atomic weight of iron
F	Faraday's constant
D_1, D_2, D_3 and D_4	deflection value of the test beam
D_{down}	the mid-deflection value of the bottom beam
D_{up}	the mid-deflection value of the top beam
i	current density
r	the original radius of the steel bar
t	time elapsed
Z	valency of the reacting electrode
η_s	the mass loss ratio or the corrosion degree of a corroded steel bar
ρ	the steel density

on the corrosion process [5,6]. Furthermore, beam behavior under the combined effects of loading and corrosion is time-dependent. To predict the service life of corroded RC structures, it is important to clarify the time-dependent behavior of the corroded beam.

Combined action of loading and corrosion was considered in the experiments by many researchers, and different current densities have been applied in the accelerated corrosion process. Experimental study by Ballim et al. [5] showed that the sustained load effect on the deflection of a RC beam could not be ignored during the corrosion process. The current density applied in the experiment carried out by Ballim et al. was 400 μA/cm^2, which could get an ideal corrosion degree in a short period of time. However, the common current density that governs the corrosion rate of actual in-service corroding concrete structures normally ranges between 0.1 and 100 μA/cm^2 [7,8]. Additionally, the nominal current density applied in the accelerated corrosion testing should be less than 200 μA/cm^2 [9]. The experiment carried out by El Maaddawy et al. [10] and Malumbela et al. [11,12] used a relatively low current density. EI Maaddawy et al. monitored the corrosion crack development and the deflection of the testing beams under the current density of approximately 150 μA/cm^2 during the testing process; moreover, results showed that the sustained load significantly reduced the initiation time of corrosion-induced cracking and slightly increased the corrosion crack's width. The results also indicated that the flexural crack induced by the sustained load could initially increase the corrosion rate of the steel bars. Malumbela et al. did a series of experiments on the beams under the current density of 189 μA/cm^2 and recorded the deflection, corrosion crack width, crack pattern, and so on. The results also suggested that effects of the sustained load could not be ignored.

It's well-known that time-dependent flexural behaviors of RC beams subjected to sustained loading or reinforcement corrosion have a direct relation to loading level or corrosion rate. However, the current densities and loading levels recorded in tests are always different from that of actual in-service structures, and the current density in the actual RC structures is always less than that applied in tests. Thus, in this paper, an experimental investigation was carried out on the structural behavior of RC beams subjected to simultaneous loading with different levels and reinforcement corrosion with different rates. Particular attention was paid to the combined effects on initiation and propagation of corrosion crack, deflection of RC beams.

2. Experimental program

2.1. Specimen preparation

Eight RC beams with the same dimensions of 150 × 200 × 2200 mm were designed and casted, as shown in Fig. 1. The flexural reinforcement consisted of two 14 mm-diameter deformed steel bars in the tension zone and two 10 mm-diameter deformed bars in the compression zone. The thickness of concrete cover was 25 mm. The shear reinforcement consisted of 6 mm diameter plain stirrups spaced at 150 mm intervals along the beam. Eight beams were divided into two groups. Three of these beams were uncorroded, which belonged to Group A, and the other five were corroded, which belonged to Group B. The tensile steel bars in Group B were extended to protrude approximately 50 mm out of the end of the specimen to allow them to be connected to the power supplies during the accelerated corrosion process. Stirrups in Group B were coated with epoxy resin to protect them from corrosion. As a further precaution, plastic wires were used to fasten the longitudinal steel bars to the stirrups. Tensile testing was carried out on the tensile bars used in the experiment. The average tested yield strength and ultimate strength of three 14 mm deformed bars were 353 MPa and 533 MPa, and the modulus was 201 GPa.

The concrete mixture proportions are given in Table 1, and the 28-day compressive strength was acquired by conducting uniaxial compressive tests on the concrete cube specimens with a length of 150 mm. Ordinary Portland cement and tap water were used in this research. Crushed gravel with continuous grading ranging from 5 mm to 20 mm was used as the coarse aggregate, and natural sand with a fineness modulus of 2.64 was used as the fine aggregate.

2.2. Sustained loading system

The three specimens in Group A were subjected to sustained loading at three different load levels. The specimens in Group B were under three different load levels and three different current densities were applied to the corroded specimens, as shown in Table 2. In order to decrease the effect of concrete creep, all the beams were loaded after 150 days of casting.

A sustained loading system was designed to study the performance of flexural members, as shown schematically in Fig. 2. The beams in the sustained loading system were tested with a four-point bending over a span of 1800 mm with a constant moment region of 600 mm. The load was applied on specimens by hanging weights on a lever beam. Two lever arms were used to amplify the hung weight to the load at the midpoint of the distributed beam. Lever arm I was used to magnify a hung weight G from point A to point B. Load N at point B equals $l_1 \cdot G$. Point A could be one of the three different holes. When the weight hung at the different holes, the value of l_1 could be 8, 9 or 10. Load F at point C was 9 times greater at point B after magnified by lever arm II, i.e. $F = 9$ N. Therefore, after magnification of two lever arms' action, the load at point C to the distributed beam could be up to 72, 81 or 90 times of the hung weight G at point A. The distribution beam distributed the load equally to two loading points placed at the ends of the middle third position marked on the top beam, and F_{py} at each loading point was equal to 0.5 F.

One or two pairs of two beams were loaded back-to-back simultaneously in the loading system, where the bottom beams were loaded with tensile face up and the top beams were loaded with

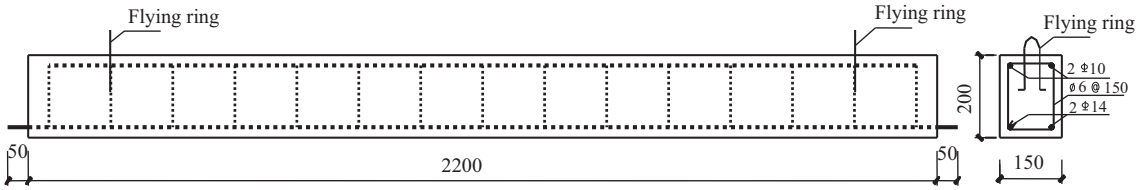

Fig. 1. Details of the test beams.

Table 1
Mixture proportions and compressive strength of concrete.

w/c	Cement (kg/m^3)	Water (kg/m^3)	Fine aggregate (kg/m^3)	Coarse aggregate (kg/m^3)	Compressive strength (MPa)
0.53	368	195	735	1103	49.7

Table 2
Loading level and current density for beams.

Beam No.	A-17-00	A-33-00	A-50-00	B-17-50	B-33-25	B-33-50	B-33-100	B-50-50
Sustained load as a percentage of ultimate capacity	17	33	50	17	33	33	33	50
Current density (μA/cm^2)	–	–	–	50	25	50	100	50

tensile face down. Two pairs of beams can be tested under the corresponding designed levels of sustained loads in the loading system. The beams of Group B were placed as bottom beams subjected to both sustained loading and reinforcement corrosion, and the beams of Group A and supplementary beams were placed as top beams without reinforcement corrosion.

To calibrate the amplification coefficient before the loading test, the hung weight G at point A was increased step by step, and the applied force F at the midpoint of the distributed beam was tested by pressure sensor at point C. The schematic calibration curve of the hung weight and the applied force is shown in Fig. 3. The curve showed good linearity. In the test, two lever arms were used to magnify the hung weight G approximately 81 times to the midpoint of the distributed beam. Considering the self-weight of the levers, the value of the load at the distributed beam's midpoint was approximately $F = 80.8\,G + 2.6$ (kN). The tested amplification coefficient agreed well with the designed value.

Based on material properties, the cracking load and the ultimate load of the uncorroded beam under four-point bending were calculated as 14.74 kN and 55.15 kN, respectively. Therefore, the load at midpoint of the distributed beam corresponding to the load levels of 17%, 33% and 50% of the designed ultimate load was 9.38 kN, 18.20 kN, and 27.58 kN, respectively. And the weight applied at point A was 0.09 kN, 0.20 kN and 0.32 kN, respectively.

2.3. Accelerated corrosion in reinforcement

The sustained loading system was placed in a pool with 3% sodium chloride solution, and the water surface was about 50 mm lower than the corroded bars in test beams of Group B. After test beams of Group B were immersed in the solution for 30 days, two tensile steel bars in each beam were connected in series to apply current with the density of 25, 50 or 100 μA/cm^2. The direction of the current was adjusted so that the tensile steel bars became the anode and a copper bar immersed in the solution served as the cathode, as shown in Fig. 2(a) and (d).

To clarify the mass loss of corroded bars, the same steel bars were embedded in 24 concrete slabs, and the slabs were casted and corroded under the same conditions as the test beams. The corroded steel bars were retrieved from the test slabs, cleaned, and weighed to determine the gravimetric mass loss at a certain time interval according to the ASTM G1-03 standard [13]. Fig. 4 shows the steel bars' measured and calculated values of corrosion degree and were determined by Faraday's law as given in Eq. (1). Fig. 4 also shows the calculated values to be in good agreement with the measured values. Therefore, ignoring the effect of sustained loading, the corrosion degree of the steel bars in the Group B beams could be predicted by Eq. (1), which is equal to the corrosion degree of steel bars in concrete slabs with the same current density and corrosion duration.

$$\eta_s = \frac{2A \cdot i \cdot t}{Z \cdot F \cdot r \cdot \rho} \tag{1}$$

where η_s is the mass loss ratio or the corrosion degree of a corroded steel bar; A is atomic weight of iron (56 g); i is current density (μA/cm^2); t is time elapsed (second); Z is valency of the reacting electrode (iron), which is 2; F is Faraday's constant (96500 A s); r is the original radius of the steel bar (cm); ρ is the steel density (7.85 g/cm^3).

2.4. Measuring techniques and instrumentation

In order to observe the crack development during the corrosion process, the test beams were coated with whitewash and the grids were drawn to the surface before being loaded in the sustained loading system. In order to determine the initiation time of corrosion cracking, the test beams were carefully inspected two or three times a week during the initial period. After that, the test beam was observed once a week.

The transverse crack, the longitudinal crack and crack width of the test beams were recorded during the corrosion process. Four dial gauges were set up for each pair of the test beams to record the mid-deflection development of the beams, as shown in Fig. 5. The value of the dial gauge was recorded two or three times a week initially and once a week after the deflection of the test beams became steady. Mid-span deflections of the two beams were calculated according to Eqs. (2) and (3).

$$D_{up} = D_3 - (D_1 + D_2)/2 \tag{2}$$

$$D_{down} = D_4 + (D_1 + D_2)/2 \tag{3}$$

where D_{up} is the mid-deflection value of the top beam; D_{down} is the mid-deflection value of the bottom beam; D_1, D_2, D_3 and D_4 are shown in Fig. 5.

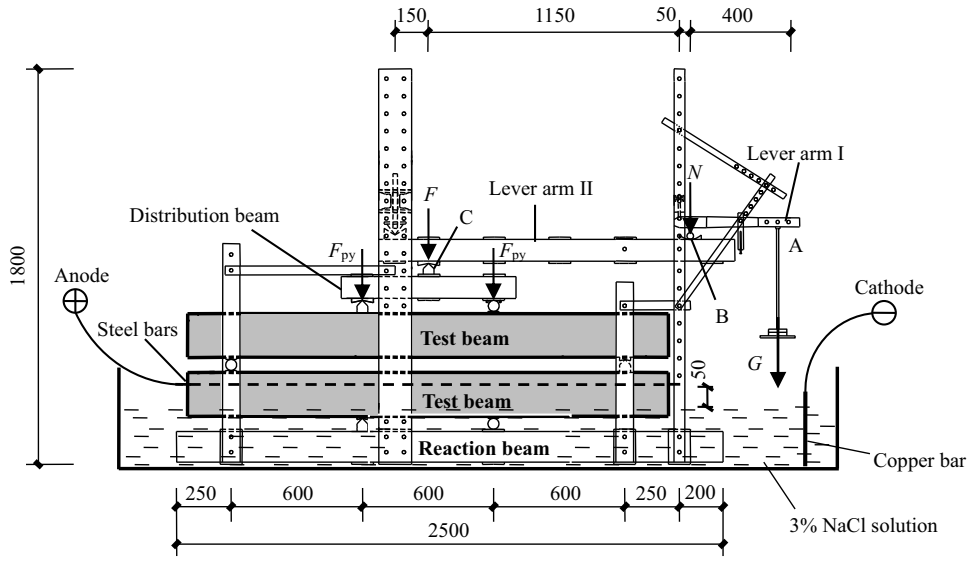

(a)

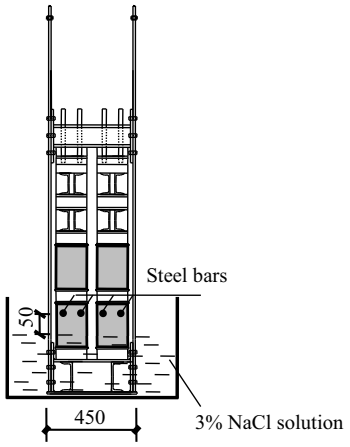

(b)

(c)

(d)

Fig. 2. Sustained loading system (Units: mm) showing: (a) Elevation, (b) Side elevation, (c) Photo of loading system, and (d) Photo of experimental site.

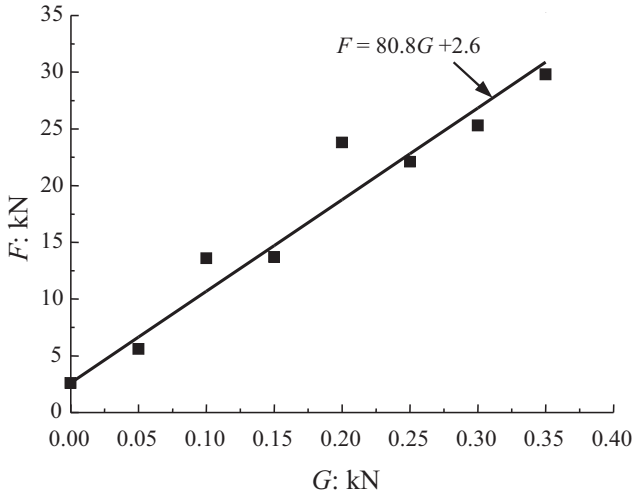

Fig. 3. Calibration curve of the sustained loading system.

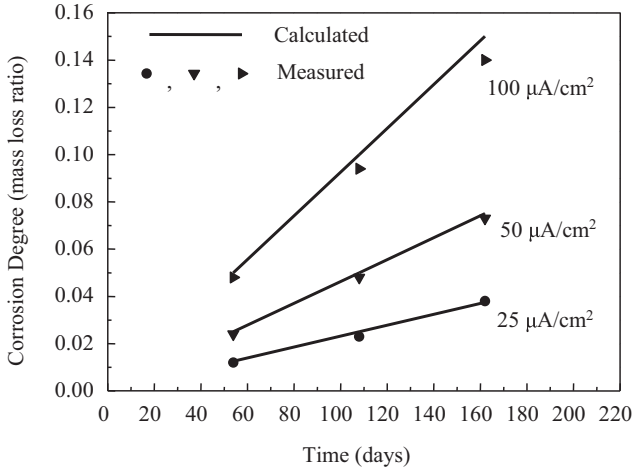

Fig. 4. Corrosion degree versus time.

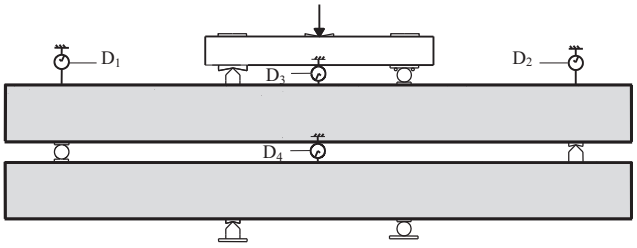

Fig. 5. Instrumentation for the deflection measurement.

3. Crack patterns and crack widths

3.1. Crack development of uncorroded beams

As control beams, three beams in Group A were loaded under different load levels. No visible flexural cracks were found on the beam with the load level of 17%. For the beams under load levels of 33% and 50%, flexural cracks formed in the direction perpendicular to the neutral axis of each beam. The maximum crack widths were 0.2 mm and 0.4 mm, respectively, and the spacing of cracks was approximately 150 mm. The flexural cracks of the specimens in Group A did not develop noticeably during the loading process. The schematic crack patterns for specimens in Group A at the age of 150 days are shown in Fig. 6.

3.2. Effect of load level on the crack development of the corroded beams

Table 2 shows specimens in Group B loaded under the different load levels and impressed with different current densities. The reinforcement corrosion process started 30 days after the specimens were loaded. Before corrosion, the behavior of specimens in Group B was similar to that in Group A.

Specimens B-17-50, B-33-50 and B-50-50 were tested under the same current density of 50 μA/cm^2 and different load levels of 17%, 33%, and 50% of the ultimate load, respectively. The details of the crack patterns for these specimens are shown in Fig. 7(a)–(c). There was no flexural crack for specimen B-17-50, which was similar with the case for specimen A-17-00 at the beginning of the test. In theory, the cracking moment of the B-17-50 beam (Fig. 7(a)) was supposed to decrease slightly with the decrease of the effective cross section of the corroded reinforcement. Although the calculated corrosion degree of specimen B-17-50 was 0.082 with a corrosion duration of 180 days, the theoretical cracking moment reduced to 4.37 kN m, and was still greater than the applied moment. Hence, no new visible flexural crack appeared during the loading process. The flexural crack patterns for specimens B-33-50 and B-50-50 were also similar to the uncorroded specimens under the same load levels.

Different from the pre-corroded beam before loading [2–4], no more flexural cracks appeared during the corrosion process after cracking at the beginning of loading, and flexural crack spacing was not influenced by the steel corrosion. A slight increase of the flexural crack width was noticed with the increasing corrosion degree, resulting from the degraded bonding behavior. The stresses of the concrete and steel tended to be uniform with the bonding degradation, which caused the crack width to increase.

Since the width of the transverse cracks increases with the increase of the load level, and the transverse cracks allow oxygen and other corrosion substances to reach the steel surface more easily, the initiation of corrosion comes sooner and wider corrosion cracks occur at the same corrosion degree [14]. The initial corrosion cracks of specimens B-17-50, B-33-50 and B-50-50 appeared on the surface on the 16th day, the 14th day and the 10th day after corrosion, respectively. According to Eq. (1), the predicted corresponding corrosion degrees were 0.007, 0.006 and 0.005, respectively. The maximum corrosion crack widths of specimens B-17-50, B-33-50 and B-50-50 were 0.2 mm, 0.3 mm, and 0.4 mm after 180-day corrosion, respectively, which are shown in Fig. 7(a)–(c). For specimens with the same corrosion degree, El Maaddawy

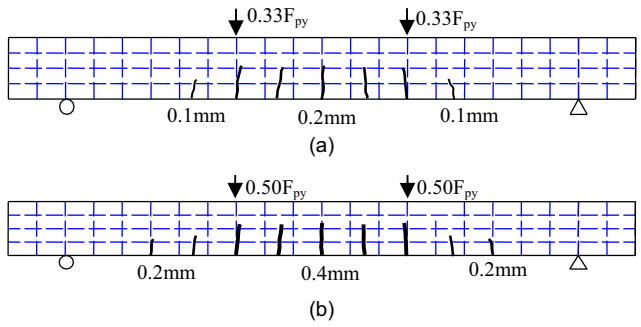

Fig. 6. Crack patterns for specimens of Group A (At the concrete age of 150 days) (a) Specimen A-33-00 (b) Specimen A-50-00.

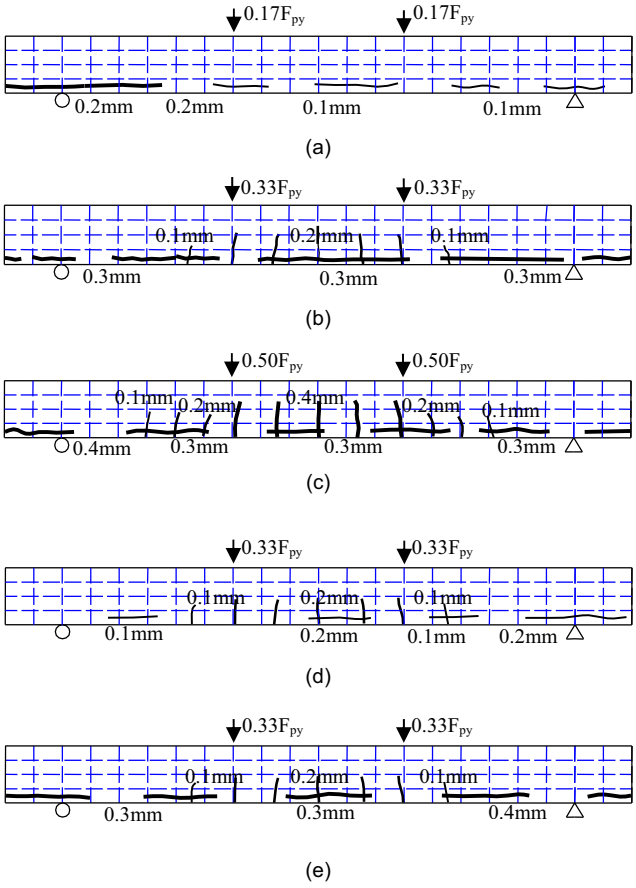

Fig. 7. Crack patterns of specimens in Group B (180 days after corrosion) (a) Specimen B-17-50 (b) Specimen B-33-50 (c) Specimen B-50-50 (d) Specimen B-33-25 (e) Specimen B-33-100.

et al. [10] and others have also found that the width of the corrosion crack increases with the increase of the load level.

3.3. Effect of applied current density on the crack development of the corroded beams

Specimens B-33-25, B-33-50 and B-33-100 were tested under the same sustained load level of 33% and different current densities of 25 μA/cm^2, 50 μA/cm^2 and 100 μA/cm^2, respectively. The transverse cracks of these three specimens were similar to specimen A-33-00, and the crack patterns for these specimens after 180 days of corrosion are shown in Fig. 7(b)–(e). The earliest visible corrosion cracks of the three specimens appeared on the 16th day, the 14th day and the 8th day after corrosion, with the corresponding corrosion degrees of 0.004, 0.006 and 0.007, respectively. The results indicated that the corrosion degree of cracking initiation increased with the increase of the applied current density. The corrosion degree for specimen B-33-100 after 45 days and specimen B-33-50 after 90 days corrosion were all theoretically 0.041, which was same as that of specimen B-33-25 after 180 days of corrosion, while the corresponding corrosion cracks widths for specimens B-33-100, B-33-50 and B-33-25 were 0.1 mm, 0.15 mm and 0.2 mm, respectively. The higher current density induced insufficient oxidation of corrosion products and a lower degree of volume expansion. These corrosion products could exude from the corrosion crack like the liquid when moisture content was high. This was demonstrated by some corrosion products found attached to the surface of the test beam near the crack. And finally, the high current density applied in the specimen would delay the initiation and propagation of corrosion cracking.

4. Deflection development of beams

4.1. Deflection development of uncorroded beams

The time-dependent deflection curves of beams in Group A are shown in Fig. 8(a). The larger initial mid-span deflection can be found in the beam with a higher load level as expected. The specimen A-17-00 was in the elastic stage under the load level of 17% and the initial mid-span deflection was only 0.24 mm. Corresponding to the increased ratio of the load, the value of the mid-span deflections should be approximately 0.48 mm and 0.72 mm by linear analysis for the specimen under the load level of 33% and 50%, respectively. However, their initial mid-span deflections were 0.58 mm and 1.17 mm respectively, much larger than the "theoretical" values. The reason was that the transverse cracks in the specimen decreased the stiffness of the beam after the load was applied.

The increase of the mid-span deflection of the uncorroded beam was mainly due to the time dependent effect, such as creep, even though the concrete age was 150 days when the beams were

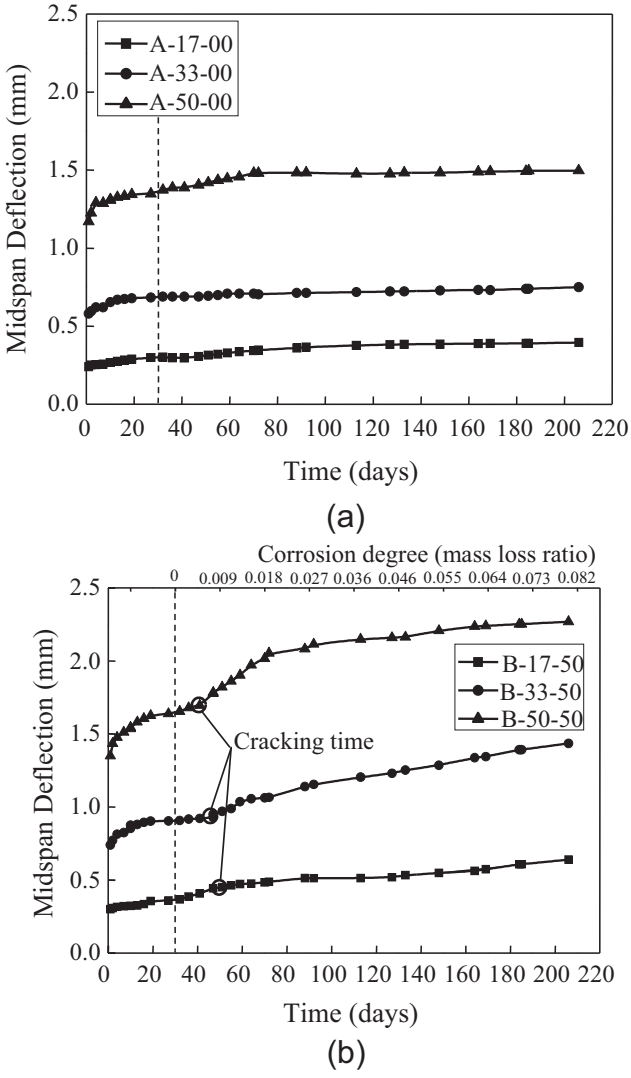

Fig. 8. Time-dependent deflection of test beams (a) Uncorroded beams in Group A and (b) corroded beams under different loads.

loaded. After a period of loading time, the creep effect on the deflection was decreased, and the growth rate of the mid-span deflection tended to slow down. After 210 days of loading, the mid-span deflection of these specimens was about 0.40 mm, 0.75 mm and 1.50 mm, which was equal to 1.8, 1.29 and 1.33 times of the initial deflection, respectively.

4.2. Effect of load levels on deflection development of corroded beams

Fig. 8(b) shows the mid-span deflections of specimens B-17-50, B-33-50 and B-50-50 which were tested under the same current density and different load levels. The deflection development curves displayed obvious characteristics of three stages under simultaneous loading and reinforcement corrosion: 1) the deflection stable development stage before the corrosion crack initiation, 2) the rapid development stage after the corrosion crack appeared followed by 3) the final stable deflection stage.

At the initial stage of the test, the behaviors of corroded specimens were similar to that of the uncorroded specimens. The initial deflection was 0.30 mm, 0.74 mm and 1.35 mm, respectively; hence, the deflection developed stably. The corrosion cracks initiated in specimens B-17-50, B-33-50 and B-50-50 on the 16th day, 14th day and 10th day after corrosion, respectively. And the mid-span deflection developed rapidly after corrosion cracks initiated, which indicated that the specimen had entered into the second stage. The reason for that was the flexural stiffness decreased, which was mainly caused by the area reduction of the rebar and the bonding degradation between steel and concrete. After that, the interface between the steel and the concrete and the corrosion cracks were filled up by the corrosion product [15]. It would decrease the bonding degradation rate and induce a slow decrease of flexural stiffness [11]. Therefore, the deflection progress entered into the third stage at about 58th day, 34th day and 40th day after corrosion for specimens B-17-50, B-33-50 and B-50-50, respectively. And the corresponding corrosion crack widths were 0.05 mm, 0.1 mm and 0.15 mm while the corrosion degrees were 0.027, 0.016 and 0.018, respectively. It is interesting to mention that during the testing process, the deflection of the corroded specimen under the load level of 50% was always about 1.2 times larger than the deflection of the corroded specimen under the load of 33% and 3.7 times larger than the deflection of the corroded specimen under the load of 17%.

In order to eliminate the creep effect, the relative deflection of the corroded beams was obtained by subtracting the deflections of the uncorroded beams from the corresponding deflections of the corroded beams at the same time under the same loading. Fig. 9 shows the relative deflection curves, which increased linearly with the corrosion degree at the beginning of corrosion. When the corrosion degree was up to about 0.009–0.018, this increasing tendency was reduced. The critical time for these two parts was at about the 40th day, 23rd day and 19th day after corrosion for specimens B-17-50, B-33-50 and B-50-50, respectively. Relative deflection curves also indicated that a higher load level would induce a larger relative deflection, even though the beams were under the same corrosion rate. This larger deflection can also be attributed to rapid propagation of corrosion cracking caused by the more sufficient oxidation and a larger volume expansion of the corrosion products.

4.3. Effect of current density on deflection development of corroded beams

Fig. 10 shows the mid-span deflections of specimens A-33-00, B-33-25, B-33-50 and B-33-100 tested under the same load level at different current densities. The initial deflections for these specimens under the same load level of 33% were 0.58 mm, 0.71 mm, 0.74 mm and 0.6 mm, respectively, due to the variation of material properties. The deflection development curves of corroded specimens also displayed noticeable characteristics of three stages under simultaneous loading and reinforcement corrosion. The initial corrosion cracks appeared in specimens B-33-25, B-33-50 and B-33-100 at about the 16th day, the 14th day and the 8th day after corrosion, respectively, and the mid-span deflection development significantly increased after the corrosion cracks appeared. Nonetheless, the mid-span deflection curve stabilized at about the 42nd day, the 34th day and the 25th day after corrosion, respectively. The corresponding corrosion degrees of specimens B-33-25, B-33-50 and B-33-100 were about 0.010, 0.016 and 0.023, respectively, and the maximum corrosion crack width was all 0.1 mm for all specimens. This suggested that the mid-span deflection increased with the increase of the applied current density during the corrosion process.

Three corroded specimens theoretically reached the same corrosion degree of 0.041 after corrosion of 45 days, 90 days and 180 days. The deflections were 1.09 mm, 1.21 mm and 1.25 mm for specimens B-33-100, B-33-50 and B-33-25 at each corresponding time, respectively. This indicated that the deflection development was inversely proportional to the current density applied to the specimen. The reason for that was the volume expansion

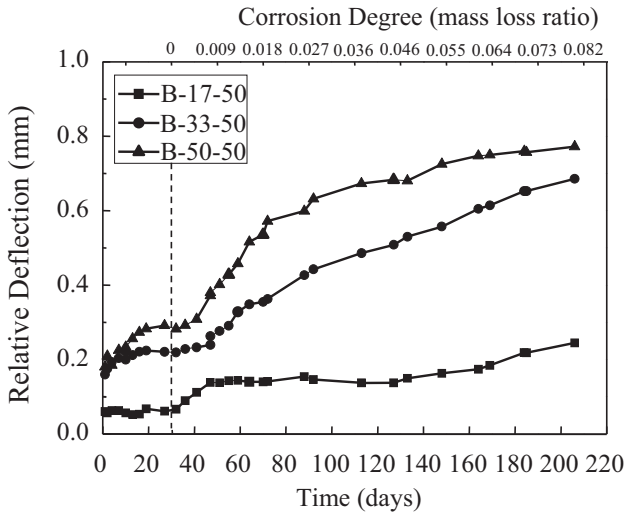

Fig. 9. Time-dependent relative deflections of corroded beams.

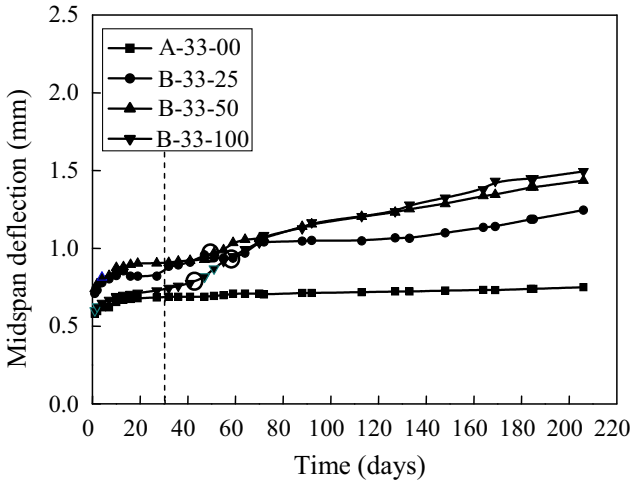

Fig. 10. Time-dependent deflections of beams under different corrosion rates.

rate of the corrosion product was related to the current density applied. Under the same surrounding conditions, low current density could let the corrosion product be oxidized more sufficiently and get a larger volume expansion rate, inducing a wider corrosion crack. It can be inferred that the measured deflection of a beam subjected to a higher current density in the lab would be less than that in a real structure under a lower current density with the same loading level and corrosion degree. To reasonably simulate the deflection development in a real structure, the applied current density in the lab should be as small as possible.

4.4. Creep effect on deflection development of beams

The deflection of the creep effect for an uncorroded beam was obtained by subtracting the instantaneous deflection from the deflection itself. Fig. 11 shows the time-dependent deflection of creep effect and how deflections increased monotonically as time progressed but at a decreasing rate.

Assuming that the beam specimens under the same ambient environment and sustained loading have a same creep effect, the corrosion effect on the deflection of a corroded beam was obtained by subtracting the deflection of the creep value of the corresponding uncorroded beam and the instantaneous deflection of itself from deflection of the corroded beam. The curves of comparison between the deflections due to creep effect and corrosion effect are shown in Fig. 12. The curves indicate that the corrosion effect will surpass the creep effect to be the principal factor of the deflection development after a period of corrosion time, except for Fig. 12(a). A similar result could be found in the experiment carried out by Malumbela et al. [16]. For specimen B-17-50 under a lower loading level, no transverse cracks were found, and oxidation of corrosion products was not so sufficient that the bonding behavior degraded slowly and corrosion effect on the deflection development surpassed creep effect at a relatively large corrosion degree. From Fig. [12], it can also be concluded that the corrosion effect cannot be ignored when calculating the deflection of the beam under simultaneous loading and reinforcement corrosion.

5. Conclusions

(1) Transverse cracks appeared under loading prior to reinforcement corrosion in the test, and the reinforcement corrosion had no obvious effect on the transverse crack spacing but a slight effect on the crack width.

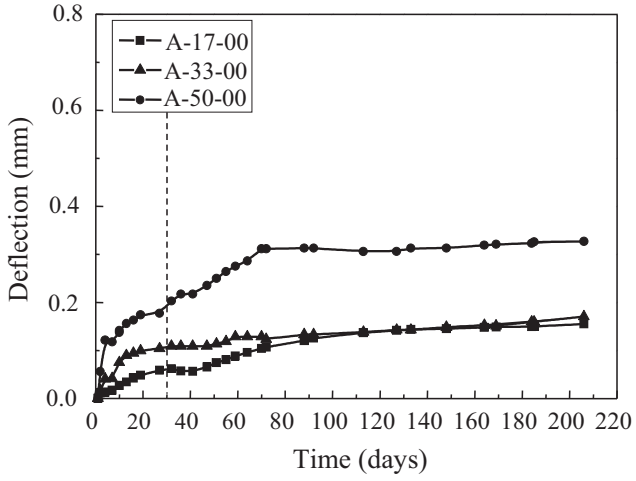

Fig. 11. Deflection due to creep effect.

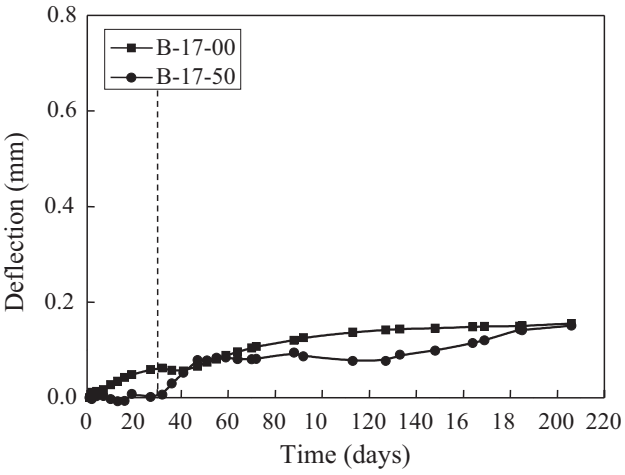

(a)

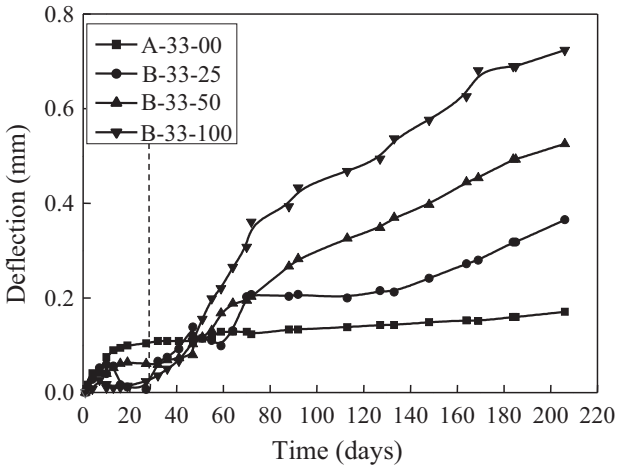

(b)

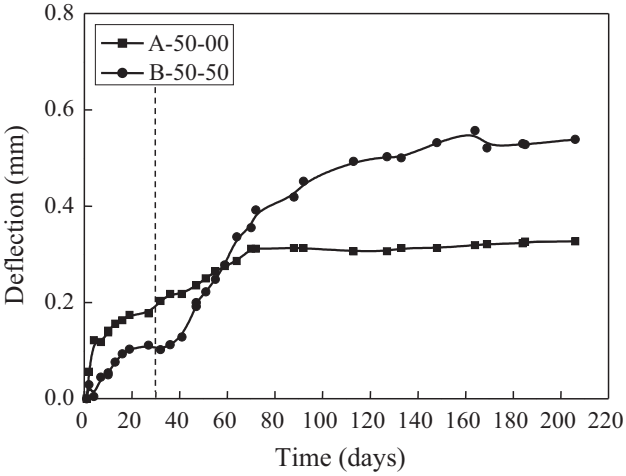

(c)

Fig. 12. Comparison between deflections due to the creep effect and corrosion effect of (a) B-17-50 and A-17-00 (b) B-33-25/50/100 and A-33-00 and (c) B-50-50 and A-50-00.

(2) The deflection development curves displayed obvious characteristics of all three stages under simultaneous loading and reinforcement corrosion. The deflection stable development stage before the corrosion crack initiation was followed by the rapid development stage. The other stable

stage of the deflection began when the interface between the steel and the concrete and corrosion cracks were filled up by the corrosion product.

(3) For the specimens under the same current density, a lower load level might delay the initiation and propagation of corrosion cracking. Furthermore, for the specimens subjected to loading at the same level, a higher current density might also delay the initiation and propagation of corrosion cracking. This delayed initiation and propagation can be attributed to more insufficient oxidation and a lower volume expansion of corrosion products.

(4) Corrosion effect cannot be ignored on the calculation of the deflection of the beams under simultaneous loading and reinforcement corrosion. At a certain corrosion degree, the beams subjected to a higher load level and a lower current density would have a larger deflection.

For RC structures under a corrosion environment, such as a marine environment, the effects of corrosion and sustained loads are two main factors influencing service life. Deterioration rates of different structural members will differ due to corrosion rate and the load level. In order to assess the structural behavior of RC structures under a corrosion environment, it's important to clarify the relationship between the sustained load and the corrosion rate of a structural member. The time-dependent flexural behavior of RC beams subjected to different loading levels and different corrosion rates in this paper can be used to investigate the performance of RC structures under simultaneous reinforcement corrosion and sustained loads, and can also help assess the service life of RC structures under the corrosion environment.

Conflicts of interest

There are no conflicts of interest.

Acknowledgement

The financial support from the National Basic Research Program of China (973 Program) (2015CB655103) and the National Natural Science Foundation of China (Grant No. 51320105013) are gratefully acknowledged.

References

[1] P.K. Mehta, Concrete Technology at the Crossroads–Problems and Opportunities, ACI Special Publication, 1994.
[2] J.G. Cabrera, Deterioration of concrete due to reinforcement steel corrosion, Cem. Concr. Compos. 18 (1) (1996) 47–59.
[3] P.S. Mangat, M.S. Elgarf, Flexural strength of concrete beams with corroding reinforcement, ACI Struct. J. 96 (1) (1999) 149–158.
[4] A.A. Torres-Acosta, S. Navarro-Gutierrez, J. Terán-Guillén, Residual flexure capacity of corroded reinforced concrete beams, Eng. Struct. 29 (6) (2007) 1145–1152.
[5] Y. Ballim, J.C. Reid, A.R. Kemp, Deflection of RC beams under simultaneous load and steel corrosion, Mag. Concr. Res. 53 (3) (2001) 171–181.
[6] L. Hariche, Y. Ballim, M. Bouhicha, et al., Effects of reinforcement configuration and sustained load on the behaviour of reinforced concrete beams affected by reinforcing steel corrosion, Cem. Concr. Compos. 34 (10) (2012) 1202–1209.
[7] C. Alonso, C. Andrade, J. Rodriguez, et al., Factors controlling cracking of concrete affected by reinforcement corrosion, Mater. Struct. 31 (7) (1998) 435–441.
[8] C. Andrade, C. Alonso, On-site measurements of corrosion rate of reinforcements, Constr. Build. Mater. 15 (2) (2001) 141–145.
[9] T.A. El Maaddawy, K.A. Soudki, Effectiveness of impressed current technique to simulate corrosion of steel reinforcement in concrete, J. Mater. Civ. Eng. 15 (1) (2003) 41–47.
[10] T.A. El Maaddawy, K.A. Soudki, T. Topper, Long-term performance of corrosion-damaged reinforced concrete beams, ACI Struct. J. 102 (5) (2005) 649–656.
[11] G. Malumbela, P. Moyo, M. Alexander, Behaviour of RC beams corroded under sustained service loads, Constr. Build. Mater. 23 (11) (2009) 3346–3351.
[12] G. Malumbela, M. Alexander, P. Moyo, Interaction between corrosion crack width and steel loss in RC beams corroded under load, Cem. Concr. Res. 40 (9) (2010) 1419–1428.
[13] ASTM. ASTM G1-03(2011) Practice for Preparing, Cleaning, and Evaluating Corrosion Test Specimens.
[14] M. Yamashita, H. Konishi, T. Kozakura, et al., In situ observation of initial rust formation process on carbon steel under Na_2SO_4 and NaCl solution films with wet/dry cycles using synchrotron radiation X-rays, Corros. Sci. 47 (10) (2005) 2492–2498.
[15] Y. Zhao, H. Ren, H. Dai, et al., Composition and expansion coefficient of rust based on X-ray diffraction and thermal analysis, Corros. Sci. 53 (5) (2011) 1646–1658.
[16] G. Malumbela, P. Moyo, M. Alexander, Longitudinal strains and stiffness of RC beams under load as measures of corrosion levels, Eng. Struct. 35 (2012) 215–227.